

# Stability and Robustness Analysis of Frequency-shaped Impedance Control for Reference Tracking and Compliant Interaction

Sehoon Oh, Hanseung Woo and Kyoungchul Kong\*

\* *Department of Mechanical Engineering, Sogang University, Seoul,  
Korea (Tel: +82-2-705-4766; e-mail: kckong@sogang.ac.kr).*

---

**Abstract:** There have been several design methodologies of impedance control without using force sensors, most of which use an observer to estimate external forces and conduct impedance control based on the observed external force. Since the external forces are estimated in a feedback way in this type of force observer-based impedance control, it has been impossible to achieve reference tracking performance when the impedance is designed low for compliant interaction. This paper proposes a novel frequency-shaped impedance control which can perform compliant motions and reference tracking simultaneously. The proposed algorithm is based on the disturbance observer design which allows a straightforward design of compliant interactive force and employs feedforward controller to compensate for the frequency bandwidth that can be sacrificed due to low impedance design. Experiments with an industrial robot verify the effectiveness of the proposed controller.

---

## 1. INTRODUCTION

Electric motors which have long been used for industrial application are now utilized to assist human powers in a more direct way; starting from the power steering system in vehicle operation and to the advanced wearable robot system, there are various applications of electric motors which interact with human in a direct way. This emerging interest in the application of the power of motor to assist human extends to power assistive wheelchairs (Oh and Hori (2013); Kloosterman et al. (2013)) and robots for co-working with human (Guizzo and Goldstein (2005)).

The control algorithms for these assistive systems have also been investigated in recent years. Such control methods include the impedance control, the natural admittance control and the compliance control. The impedance control (Hogan (1985); Culmer et al. (2010)), which is usually used in rehabilitation robotics, controls robotic manipulators so that the human (i.e., patients) can follow a motion trajectory for rehabilitation. The natural admittance control (Dohring and Newman (2003)) is a method to control a responsive force of an end-effector maintaining its passivity. The natural admittance control is adequate for robotic systems that actively contact an object (e.g., atomic force microscopy). On the other hand, the typical compliance control methods require the measurements of interaction forces exerted by the human (Caccavale et al. (2005)).

Force sensors, such as strain-gauges and force-sensitive resistors, can be used for this purpose. For more accurate measurement, a sensor fusion method is often accompanied (Garcia et al. (2008)). In recent years, many efforts have

been made to develop compliance control methods without force sensors (Shibata and Murakami (2012); Mitsantisuk et al. (2012); Bickel and Tomizuka (1995)). For this purpose, the disturbance observer (DOB) has been utilized since it estimates the exogenous disturbance without any force sensor (Umeno and Hori (1991)).

Meanwhile, this type of force sensor-less impedance control sacrifices the sensitivity of the feedback loop for the compliance of the system, since the external force is observed through the feedback loop (Oh et al. (2014b)). This prevents the controller to achieve precise reference tracking performance, as the high sensitivity function to make the system compliant deteriorates the tracking performance. Compliance and reference tracking are conflicting requirements that cannot be implemented on a force sensor-less system at the same time; when a controller is designed to guarantee the compliance of a system for assistive functionality, the output position or velocity of the assistive system is driven only by human force, and the system cannot move by itself when there is no human input.

However, there are cases when the compliance and reference tracking are required for assistance of human, e.g., systems that conduct pre-defined tasks all by themselves when there is no human interaction, but present compliance when there is any human interaction to guarantee human's safety. For example, automatic doors usually open and close without human interactions, but when a human is in touch with a door it should be able to provide compliance. Industrial robots can be another example of this case. In these cases, the system should be able to exhibit compliance and reference tracking at the same time, which is not an easy task since compliance requires low impedance and the reference tracking requires high impedance.

---

\* This work was supported by the National Research Foundation of Korea (NRF) grant funded by the Korea government (MSIP) (NRF-2012R1A1A1008271).

This paper proposes an algorithm that satisfies these conflicting requirements and thus will open a way to assistive devices that have enough compliance while performing their own tasks. To this end, this paper focuses on DOB design which can facilitate both reference tracking (when used as a feedback controller) and safe human-robot interaction (when implemented as an observer). The achievements of such conflicting objectives are possible by designing a filter, called  $Q$  filter, in different ways. For the reference tracking, the  $Q$  filter is to be designed as a lowpass filter such that the estimated disturbance is fed back into the system and rejected. When the DOB is utilized to achieve compliant interaction, the  $Q$  filter may be designed to have a phase shift of 180 degrees such that the closed-loop system becomes sensitive to the disturbance.

In this paper, the  $Q$  filter is designed synthesizing these two different approaches such that both the reference tracking and the compliant interaction are guaranteed in different frequency ranges. The proposed method results in a non-minimum phase  $Q$  filter, and thus the stability issue becomes more critical compared to the typical DOB-controlled systems. The stability criterion of the proposed method and the design approaches for the associated feedback and feedforward controllers are introduced in this paper also. The proposed methods are implemented into a robot arm and verified by experimental results.

This paper is organized as follows. The basic control framework of the FSIC is introduced in Section 2. The details of FSIC is explained, and design approach to achieve frequency-shaped low impedance and the robust stability are analyzed in Section 3. Experimental results for the verification of the proposed method are given in Section 4.

## 2. FREQUENCY-SHAPED IMPEDANCE CONTROL FOR REFERENCE TRACKING AND COMPLIANT INTERACTION

Basically, any impedance control design that does not use force sensors sacrifices the reference tracking performance for compliant interaction, i.e., the sensitivity function must increase to reduce the impedance against external forces. The reference tracking performance and impedance (or, compliance) is a trade-off and cannot be achieved at the same time using any linear time invariant controller (Oh et al. (2014b)).

This paper addresses this problem by utilizing different frequency bands for reference tracking and impedance respectively. Since compliance should be guaranteed only for the interaction with humans, and the frequency of the human interaction forces is ranged in a certain band (e.g., from several tenth Hertz up to several Hertz), low impedance needs to be achieved in that frequency band.

On the other hand, high impedance should be guaranteed for the low frequency range where the reference tracking is prioritized. This difference in the focused frequency bands is utilized in the proposed control algorithm. Fig. 1 shows how to utilize the frequency band to achieve the conflicting control purposes; the proposed control prioritizes the reference tracking performance in the low

frequency range, and compliance interaction against the external force should be achieved in the middle frequency range. In the high frequency range where the modeling error and noises are exhibited dominantly, the controller should be designed mainly to achieve the robust stability.

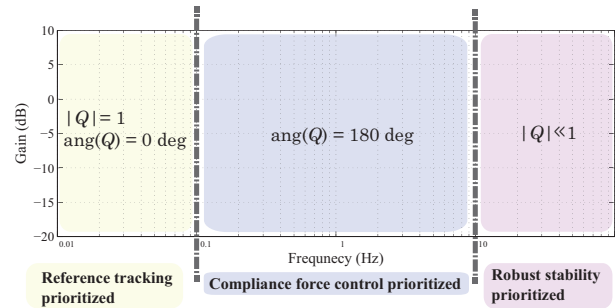


Fig. 1. Frequency bands for each control purpose

DOB is employed in this paper, since it can achieve the conflicting control purposes based on the frequency range. The  $Q$  filter which has been designed just for the reference tracking and the robust stability in the DOB, can be used for the impedance design too. Fig. 1 illustrates the guide line of the  $Q$  filter design for the reference tracking and impedance control; in the low frequency range where the tracking performance should be prioritized, the magnitude of the  $Q$  filter should be 1 and its phase should be 0 degrees, while in the middle frequency range where the impedance control is of the main interest, the phase of  $Q$  filter should be 180 degrees. The magnitude of  $Q$  filter should be reduced in the high frequency range to guarantee the robust stability and attenuate the effect of sensor noises.

This is the main idea of the proposed Frequency-Shaped Impedance Control (FSIC) which can achieve frequency-shaping of the impedance control and reference tracking. The detailed design methodology is given in the following sections.

The bandwidth of the reference tracking may be deteriorated due to the low impedance in the middle frequency range. However, this can be addressed using the feedforward control since it can enhance the frequency bandwidth of the tracking control. In order to incorporate the disturbance observer and the feedforward controller at the same time, Two-degree-of-freedom (TDOF) control (Umeno and Hori (1991)) is employed and modified in this paper. The advantage of FSIC is its practicalness; the debugging and tuning of the proposed control can be done with ease since the  $Q$  filter design is the main control parameter.

In this paper, the plant that is considered in the design of the proposed control is limited in the stable second-order system which has one integrator, since this is the most widely used plant model of a rigid body with one degree of freedom. However, the design methodology and stability criteria proposed in this paper can be extended to more complicated system.

### 3. FREQUENCY-SHAPED IMPEDANCE CONTROL BY DESIGN OF $Q$ FILTER IN DISTURBANCE OBSERVER

#### 3.1 Two-degree-of-freedom Control to Achieve Compliant Interaction with Reference Tracking

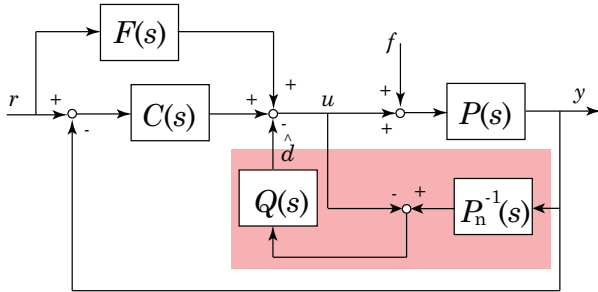


Fig. 2. Basic form of Two-degree-of-freedom (TDOF) control with disturbance observer

Fig. 2 is the basic form of TDOF control where  $C(s)$  is the feedback control,  $F(s)$  is the feedforward control,  $P_n^{-1}(s)$  is the nominal inverse model of the plant  $P(s)$ , and  $Q(s)$  is the  $Q$  filter of the disturbance observer. The shaded section is the DOB.

The main functionality of the DOB is the design of the sensitivity function;  $Q$  filter in the DOB can modify the sensitivity function as  $1-Q(s)$ , and external disturbance is eliminated up to the frequency bandwidth of the  $Q$  filter. The DOB nominalizes the plant  $P(s)$  into the nominal model  $P_n(s)$  in the frequency bandwidth of the  $Q$  filter. Feedback controller  $C(s)$  can be designed based on the nominal model. The feedforward control  $F(s)$  can be designed based on the nominal model to improve frequency bandwidth, which allows to design the reference tracking performance and the disturbance response performance independently.

The proposed FSIC exploits these features of TDOF to realize compliant motions while the tracking performance is not significantly deteriorated.

#### 3.2 $Q$ Filter Design for Frequency-shaped Compliant Motion

$Q$  filter, which is the key design factor in DOB, is usually designed using a low pass filter. In the case of a first order plant such as a plant with a torque input and velocity output,  $Q$  filter can be designed as a first order low pass filter as in (1).

$$Q_{\text{conv}}(s) = \frac{1}{\tau_q s + 1}, \quad (1)$$

where  $\tau_q$  determines the frequency bandwidth of the sensitivity function. This  $Q$  filter design implies that the impedance is designed only by  $\tau_q$ , which restricts the conventional DOB to achieve various impedance characteristics.

In order to provide a general framework to design various impedance utilizing DOB, Force Sensor-less Power Assist Control (FSPAC) has been proposed, which is illustrated in Fig. 3 (Oh et al. (2014b)), where  $P_M$  indicates the model impedance that the impedance characteristic of

the plant is to follow,  $A$  is the feedback controller for impedance tracking, and  $Q_i$  and  $Q_o$  are two low pass filters to determine the frequency bandwidth and guarantee the robust stability.

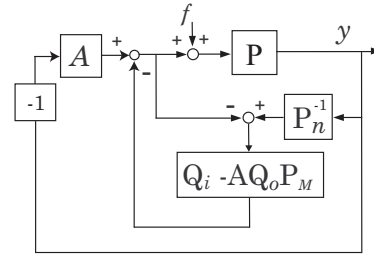


Fig. 3. Force sensor-less power assist control(FSPAC)

However, FSPAC only takes into consideration impedance design against exogenous human force, and the reference tracking performance is not considered. In order to incorporate the impedance design and tracking performance, a comprehensive design methodology based on TDOF control is proposed in this paper.

In the analysis of FSPAC, it was revealed that the equivalent  $Q$  filter of FSPAC, which is  $Q_i - A Q_o P_M$  in Fig. 3, has negative phase characteristic to achieve compliant reaction. Taking this characteristic into consideration, a novel  $Q$  filter is designed here as (2).

$$Q_{\text{imp}}(s) = \frac{-\tau_u s + 1}{\tau_l s + 1} \frac{1}{\tau_q s + 1}, \quad (2)$$

which has three parameters:  $\tau_q$ ,  $\tau_u$  and  $\tau_l$ .

$\tau_q$  works the same as the  $\tau_q$  of the conventional  $Q$  filter in (1) which determines the high cut-off frequency.  $\frac{1}{\tau_u}$  (rad/sec) is the frequency where the phase shifts from 0 to -180 degrees, and the ratio of  $\frac{\tau_u}{\tau_l}$  is the amount of the gain increase in the frequency range from  $\frac{1}{\tau_u}$  (rad/sec) to  $\frac{1}{\tau_q}$  (rad/sec). This novel  $Q$  filter to achieve the frequency-shaped impedance is called impedance shaping (IS)  $Q$  filter in this paper.

Fig. 4 is the frequency characteristic of the  $Q$  filters, where  $\tau_q = \frac{1}{2\pi \times 3}$ ,  $\tau_l = \frac{1}{2\pi \times 0.7}$ ,  $\tau_u = \frac{1}{2\pi \times 0.5}$ . The curves labelled with "filter for compliance" represent the frequency response of a filter  $\frac{-\tau_u s + 1}{\tau_l s + 1}$  in the impedance shaping  $Q$  filter. In the figure, the phase of the filter for compliance start shifting from 0 degree around  $\frac{1}{\tau_u}$  (rad/sec), and it reaches to -180 degrees around  $\frac{1}{\tau_l}$  (rad/sec), which brings the negative phase characteristic into the impedance shaping  $Q$  filter.

In the design of the impedance shaping  $Q$  filter, the frequency at which the compliant motion starts is determined by  $\tau_u$  at first. The gain increase (i.e.,  $\frac{\tau_u}{\tau_l}$ ) can modify the amount of the compliance, and  $\tau_l$  is determined by this. Lastly,  $\tau_q$  is designed to determine the bandwidth of the sensitivity function in the high frequency range, in the same way the conventional  $Q$  filter is designed. It is found that the all pass filter, in which  $\tau_u = \tau_l$  can be utilized as the impedance shaping  $Q$  filter, too (Oh et al. (2014a)).

To further discuss how the impedance shaping  $Q$  filter affects the whole system, the changes in the sensitivity

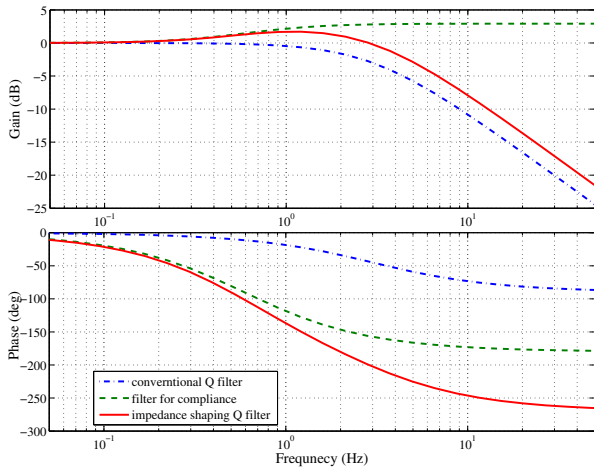


Fig. 4. Frequency characteristic of the proposed impedance shaping  $Q$  filter

function is discussed, since the sensitivity function is a powerful representation way to describe how  $Q$  filter works. Sensitivity functions with and without disturbance observer are calculated as (3) and (4).

$$S_{fb} = \frac{1}{1 + CP} \quad (\text{without disturbance observer}) \quad (3)$$

$$S_{tdof} = \frac{1 - Q}{1 + CP} \quad (\text{with disturbance observer}) \quad (4)$$

The frequency characteristics of the sensitivity functions for a plant given in (5), are shown in Fig. 5, where the inertia  $J$  is set to 0.00892, and the damping  $B$  is set to 0.0625. Notice that the nominal model of a plant is assumed to be the same as the actual dynamics of the plant in this discussion. The modeling error issues will be discussed in the following section. The position feedback controller  $C$  is designed using the PD control with the proportional gain set to 3 and the derivative gain set to 1.

$$P(s) = \frac{1}{Js^2 + Bs} \quad (5)$$

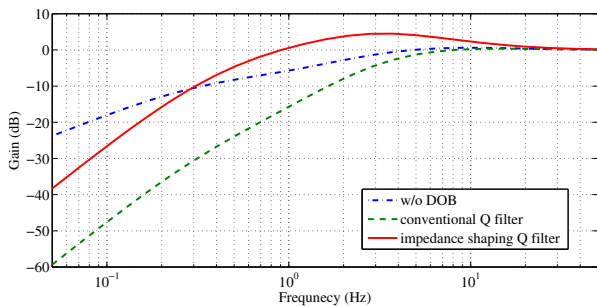


Fig. 5. Sensitivity function by the proposed impedance DOB feedback

In Fig. 5, the sensitivity function under TDOF control (the dashed line) shows lower gain characteristics than the feedback-only control (the chained line), while the proposed control with the impedance shaping  $Q$  filter shows high sensitivity in the middle frequency range (the solid line).

On the other hand, the sensitivity function of the proposed controller is still lower than the feedback-only controller in

the low frequency range, which means the proposed controller has better tracking performance than the feedback-only control without DOB.

### 3.3 Robust Stability Analysis

Since the impedance against external forces by FSIC is based on the disturbance observer which uses a nominal model of the target plant, the robustness against the modeling error should be provided. Usually the robustness is evaluated using the small gain theorem to guarantee the robust stability (Doyle et al. (1992)).

When the plant with the uncertainty is given as (6), the closed loop system is stable when it meets the criterion of (7), where  $P_n(s)$  is the nominal plant model,  $\Delta(s)$  is the uncertainty, and  $T(s)$  is the complementary sensitivity function.

$$P(s) = P_n(s) (1 + \Delta(s)) \quad (6)$$

$$\|T(s)\Delta(s)\|_\infty < 1 \quad (7)$$

In order to apply the small gain theorem to FSIC, the complimentary sensitivity function, which is defined as the transfer function from the input right after the uncertainty  $\Delta(s)$  to the output to the uncertainty is derived using Fig. 6.

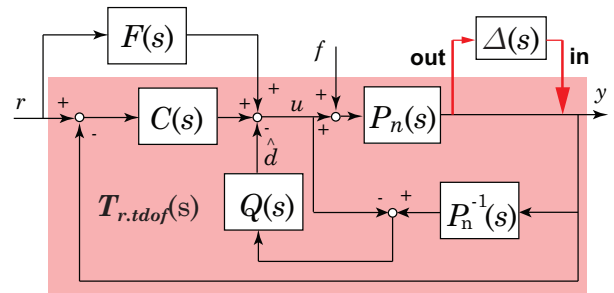


Fig. 6. Complimentary sensitivity function for robust stability analysis

The derived complimentary sensitivity function is given in (9). Compared with the complimentary sensitivity function with the usual feedback-only control given in (8),  $Q$  filter is added in the numerator in the FSIC case. Notice that this complimentary sensitivity function is the same with that of TDOF control since FSIC has the same controller framework with TDOF control.

$$T_{r.fb} = \frac{CP_n}{1 + CP_n} \quad (8)$$

$$T_{r.tdof} = \frac{CP_n + Q}{1 + CP_n} \quad (9)$$

The change in this complimentary sensitivity function by  $Q$  filters is shown in Fig. 7. At first, the complimentary sensitivity function without the disturbance observer is shown, and the complimentary sensitivity functions with two different types of disturbance observer are shown: the first is with the conventional  $Q$  filter design shown in Fig. 4, the second is with the impedance shaping  $Q$  filter shown in Fig. 4.

TDOF control with the conventional disturbance observer raises the gain of the complimentary sensitivity function compared with the feedback-only case. The gain of FSIC is larger than the gain of conventional TDOF control in the frequency range that is designed to be compliant against the external forces.

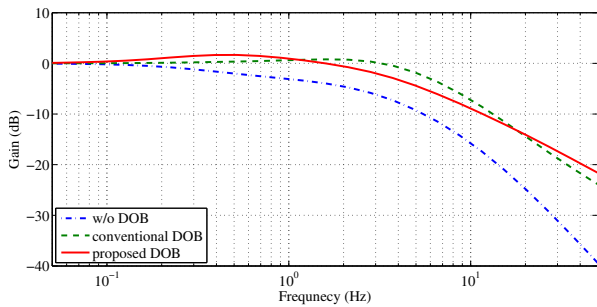


Fig. 7. Complimentary sensitivity function for robust stability analysis

This fits to the general knowledge that the sensitivity to the external forces is also the sensitivity to the modeling error, which leads to the fact that there are limits to the impedance that can be achieved by FSIC due to this robust stability problem.

#### 4. EXPERIMENTAL VERIFICATION OF FREQUENCY-SHAPED IMPEDANCE CONTROL

##### 4.1 Experimental Setup

The proposed method was verified by experimental results with a three-link robot shown in Fig. 8, which is driven by three AC motors of 400W. The joints and the motors are connected by a belt which introduces large nonlinearity due to its friction and backlash, while the motor has inherent nonlinearity in the current-torque relationship. The following experiments verify that FSIC can work effectively in spite of this nonlinearity.

Only the second joint was controlled using FSIC, and other two joints were locked in order not to affect the motion of the second joint, which is practical enough to validate the effectiveness of the proposed controller design. The parameters of the  $Q$  filters were set to  $\tau_q = \frac{1}{2\pi \times 3}$ ,  $\tau_l = \frac{1}{2\pi \times 0.7}$ ,  $\tau_u = \frac{1}{2\pi \times 0.5}$ . The feedback controller in Fig. 2 was designed as a PD control with the gains  $K_p = 3$  and  $K_d = 1$ . The nominal model of the arm was set to  $J_n = 0.00892$  and  $B_n = 0.0625$ .

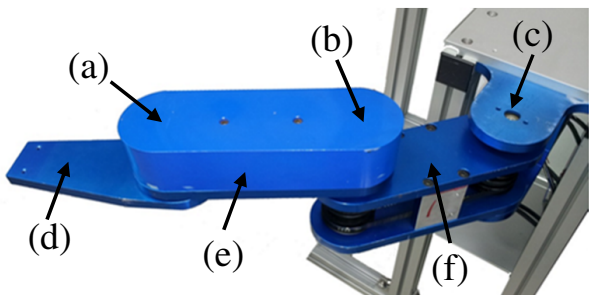


Fig. 8. Experimental setup; (a), (b), (c) are joints with actuators and (d), (e), (f) are robot frames

##### 4.2 Verification of Frequency-Shaped Impedance

The impedance of the robot arm with FSIC is evaluated by experiments. In order to apply the regulated external forces, additional motor torques with different frequencies were added as external forces. The output positions of the robot arm were evaluated to examine how the impedance of the robot arm changed according to the frequency by the proposed FSIC.

Five types of external forces with different frequencies of 0.1Hz, 0.4Hz, 0.7Hz, 1Hz and 2Hz with the same magnitude were applied. Fig. 9 shows the angles of the robot arm with and without FSIC, which reveals how FSIC can change the response of the robot arm against the external force.

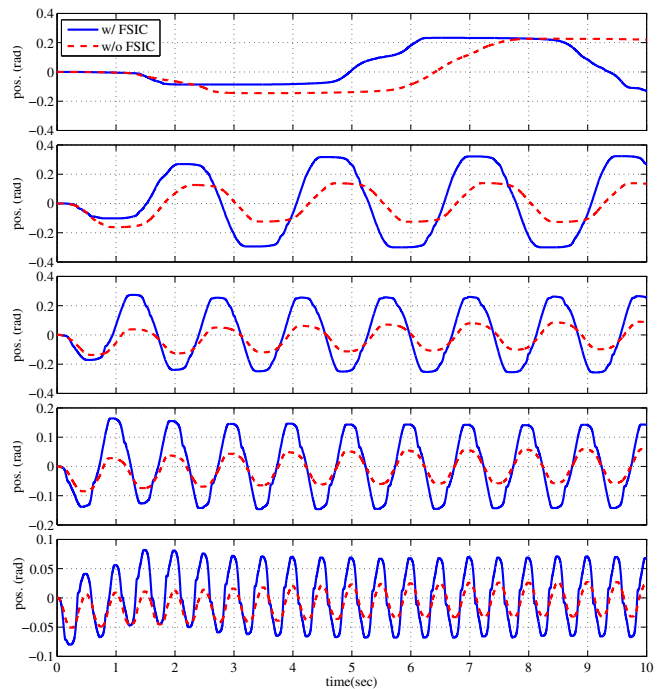


Fig. 9. Angle output against the external force. External forces are with 0.1Hz, 0.4Hz, 0.7Hz, 1Hz and 2Hz.

The solid line which is the response by FSIC exhibits similar response to the response without FSIC at low frequency range of 0.1Hz. As the frequency increases, however, the difference between two references becomes remarkable, which indicates that the robot arm moves more compliantly responding human interactive forces under FSIC. The results with these different frequencies validates that FSIC can design the desired compliance according to the frequency range of the human interactive forces.

##### 4.3 Reference Tracking Performance Evaluation

In addition to frequency-shaped impedance for compliant interaction, the reference tracking performance should be verified through experiments. Since the impedance was set low for the middle frequency range and high for the low frequency range as shown in Fig. 9, disturbance in the low frequency range such as the friction force can be rejected by DOB. Namely, FSIC can distinguish the external forces

based on their frequency ranges and effectively reject the friction force to achieve good tracking performance while it moves compliantly when the human force is applied.

Experiments were conducted to verify this feature of FSIC. Fig. 10 is the result of the experiments, where angle references with four different frequencies were applied to the robot arm, and the tracking performance was evaluated. Two cases are compared: one with the feedforward control, and the other is without the feedforward control. In both cases, FSIC is implemented. Tracking performance without the feedforward control was deteriorated at 0.4Hz and 0.7Hz, where the low impedance was implemented by the impedance shaping  $Q$  filter. With the feedforward control, however, the performance was recovered. This experiment verifies that the feedforward control in FSIC achieves high tracking performance in spite of the compromised high sensitivity by the low impedance.

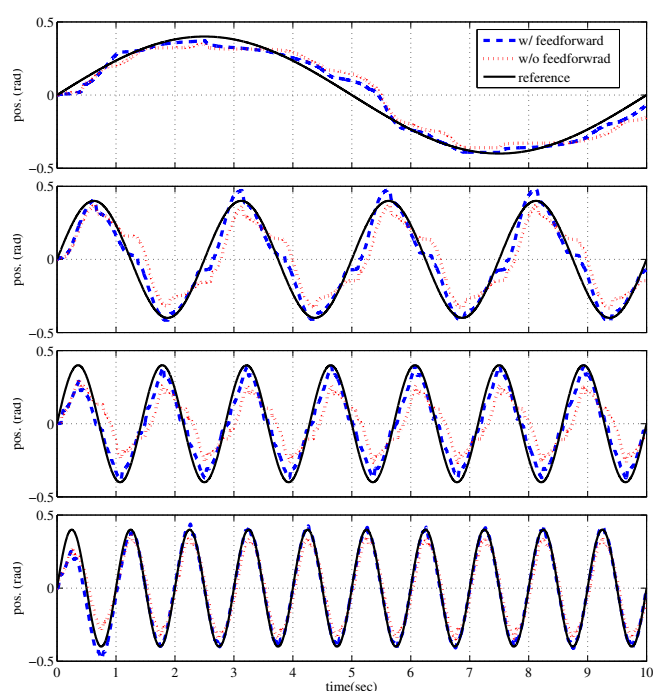


Fig. 10. Angle output with the sinusoidal reference signal with the frequencies of 0.1Hz, 0.4Hz, 0.7Hz and 1Hz.

## 5. CONCLUSION

In this paper, Frequency-shaped Impedance Control (FSIC) is proposed, and its design method and robust stability are analyzed. Since FSIC can reduce the impedance of a system in a certain frequency range, while it holds high impedance in other frequency range, it can achieve compliant interaction and tracking performance simultaneously, which is the most required characteristic for robots which need to conduct certain tasks autonomously while guaranteeing safety in the case of interaction with human.

## REFERENCES

Bickel, R. and Tomizuka, M. (1995). Disturbance observer based hybrid impedance control. In *American Control Conference, 1995. Proceedings of the*, volume 1, 729 – 733 vol.1. doi:10.1109/ACC.1995.529346.

Caccavale, F., Natale, C., Siciliano, B., and Villani, L. (2005). Integration for the next generation: embedding force control into industrial robots. *Robotics Automation Magazine, IEEE*, 12(3), 53 – 64. doi:10.1109/MRA.2005.1511869.

Culmer, P., Jackson, A., Makower, S., Richardson, R., Cozens, J., Levesley, M., and Bhakta, B. (2010). A control strategy for upper limb robotic rehabilitation with a dual robot system. *Mechatronics, IEEE/ASME Transactions on*, 15(4), 575–585. doi:10.1109/TMECH.2009.2030796.

Dohring, M. and Newman, W. (2003). The passivity of natural admittance control implementations. In *Robotics and Automation, 2003. Proceedings. ICRA '03. IEEE International Conference on*, volume 3, 3710–3715. IEEE.

Doyle, J., Francis, B., and Tannenbaum, A. (1992). *Feedback Control Theory*, volume 134. Macmillan New York.

Garcia, J., Robertsson, A., Ortega, J., and Johansson, R. (2008). Sensor fusion for compliant robot motion control. *Robotics, IEEE Transactions on*, 24(2), 430 – 441. doi:10.1109/TRO.2008.918057.

Guizzo, E. and Goldstein, H. (2005). The rise of the body bots [robotic exoskeletons]. *IEEE Spectr.*, 42(10), 50–56. doi:10.1109/MSPEC.2005.1515961.

Hogan, N. (1985). Impedance control: An approach to manipulation: Part I applications. *Journal of dynamic systems, measurement, and control*, 107(2), 17.

Kloosterman, M.G., Snoek, G.J., van der Woude, L.H., Buurke, J.H., and Rietman, J.S. (2013). A systematic review on the pros and cons of using a pushrim-activated power-assisted wheelchair. *Clinical Rehabilitation*, 27(4), 299–313. doi:10.1177/0269215512456387.

Mitsantisuk, C., Ohishi, K., and Katsura, S. (2012). Estimation of action/reaction forces for the bilateral control using kalman filter. *Industrial Electronics, IEEE Transactions on*, 59(11), 4383 –4393. doi:10.1109/TIE.2011.2173092.

Oh, S. and Hori, Y. (2013). Disturbance attenuation control for power-assist wheelchair operation on slopes. *Control Systems Technology, IEEE Transactions on*, in process. doi:10.1109/TCST.2013.2265396.

Oh, S., Woo, H., and Kong, K. (2014a). Frequency-shaped impedance control for safe human–robot interaction in reference tracking application. *Mechatronics, IEEE/ASME Transactions on*, (in press). doi:10.1109/TMECH.2014.2309118.

Oh, S., Kong, K., and Hori, Y. (2014b). Design and analysis of force-sensor-less power-assist control. *Industrial Electronics, IEEE Transactions on*, 61(2), 985–993. doi:10.1109/TIE.2013.2270214.

Shibata, T. and Murakami, T. (2012). Power-assist control of pushing task by repulsive compliance control in electric wheelchair. *Industrial Electronics, IEEE Transactions on*, 59(1), 511 –520. doi:10.1109/TIE.2011.2146210.

Umeno, T. and Hori, Y. (1991). Robust speed control of dc servomotors using modern two degrees-of-freedom controller design. *Industrial Electronics, IEEE Transactions on*, 38(5), 363 –368. doi:10.1109/41.97556.